ARMY RESEARCH LABORATORY

Effect of Initial Microstructure on the Microstructural Evolution and Joint Efficiency of a WE43 Alloy During Friction Stir Welding

by S. Palanivel, R. S. Mishra, B. Davis, R. DeLorme, K. J. Doherty and K. C. Cho

ARL-RP-423 **April 2013**

A reprint from *TMS 2013 142nd Annual Meeting and Exhibition, Supplemental Proceedings,* San Antonio, TX, 3 March 2013.

NOTICES

Disclaimers

The findings in this report are not to be construed as an official Department of the Army position unless so designated by other authorized documents.

Citation of manufacturer's or trade names does not constitute an official endorsement or approval of the use thereof.

Destroy this report when it is no longer needed. Do not return it to the originator.

Army Research Laboratory
Aberdeen Proving Ground, MD 21005-5069

ARL-RP-423 **April 2013**

Effect of Initial Microstructure on the Microstructural Evolution and Joint Efficiency of a WE43 Alloy During Friction Stir Welding

S. Palanivel and R. S. Mishra
University of North Texas

B. Davis and R. DeLorme
Magnesium Elektron North America Inc.

K. J. Doherty and K. C. Cho
Weapons and Materials Research Directorate, ARL

A reprint from the *TMS 2013 142nd Annual Meeting and Exhibition, Supplemental Proceedings,* San Antonio, TX, 3 March 2013.

REPORT DOCUMENTATION PAGE

Form Approved
OMB No. 0704-0188

1. REPORT DATE *(DD-MM-YYYY)*	2. REPORT TYPE	3. DATES COVERED (From - To)
April 2013	Reprint	May 2010–November 2012

4. TITLE AND SUBTITLE
Effect of Initial Microstructure on the Microstructural Evolution and Joint Efficiency of a WE43 Alloy During Friction Stir Welding

5a. CONTRACT NUMBER

5b. GRANT NUMBER

5c. PROGRAM ELEMENT NUMBER

6. AUTHOR(S)
S. Palanivel,[*] R. S. Mishra,[*] B. Davis,[†] R. DeLorme,[†] K. J. Doherty, and K. C. Cho

5d. PROJECT NUMBER

5e. TASK NUMBER

5f. WORK UNIT NUMBER

7. PERFORMING ORGANIZATION NAME(S) AND ADDRESS(ES)
U.S. Army Research Laboratory
ATTN: RDRL-WMM-F
Aberdeen Proving Ground, MD 21005-5069

8. PERFORMING ORGANIZATION REPORT NUMBER
ARL-RP-423

9. SPONSORING/MONITORING AGENCY NAME(S) AND ADDRESS(ES)

10. SPONSOR/MONITOR'S ACRONYM(S)

11. SPONSOR/MONITOR'S REPORT NUMBER(S)

12. DISTRIBUTION/AVAILABILITY STATEMENT
Approved for public release; distribution is unlimited.

13. SUPPLEMENTARY NOTES
A reprint from *TMS 2013 142nd Annual Meeting and Exhibition, Supplemental Proceedings*, San Antonio, TX, 3 March 2013.
[*]Center for Friction Stir Processing, University of North Texas, Denton, TX 76203
[†]Magnesium Elektron North America Inc., Madison, IL 62060

14. ABSTRACT
The initial microstructure plays an important role in determining the spatial and temporal evolution of the microstructure during friction stir welding (FSW). The overall kinetics of microstructural evolution is location sensitive and the effect of the process strain, strain rate and thermal cycle creates complexities. In the present study, magnesium based WE43 alloy has been welded employing two different welding conditions. Joint efficiency has been subsequently evaluated. The results have been correlated with detailed microstructural information obtained from SEM and OIM-EBSD. The influence of microstructural evolution on strength has been analyzed. This framework provides an approach to maximize joint efficiency.

15. SUBJECT TERMS
friction stir welding, strain rate, dynamic recrystallization, joint efficiency, stir zone (SZ)

16. SECURITY CLASSIFICATION OF:			17. LIMITATION OF ABSTRACT	18. NUMBER OF PAGES	19a. NAME OF RESPONSIBLE PERSON
a. REPORT	b. ABSTRACT	c. THIS PAGE			K. J. Doherty
Unclassified	Unclassified	Unclassified	UU	14	19b. TELEPHONE NUMBER (*Include area code*) 410-306-0871

Friction Stir Welding and Proceesing VII
Edited by: Rajiv Mishra, Murray W. Mahoney, Yutaka Sato, Yuri Hovanski, and Ravi Verma
TMS (The Minerals, Metals & Materials Society), 2013

EFFECT OF INITIAL MICROSTRUCTURE ON THE MICROSTRUCTURAL EVOLUTION AND JOINT EFFICIENCY OF A WE43 ALLOY DURING FRICTION STIR WELDING

S. Palanivel[1], R.S. Mishra[1], B. Davis[2], R. DeLorme[2], K.J. Doherty[3], K.C. Cho[3]
[1]Center for Friction Stir Processing, Department of Materials Science and Engineering, University of North Texas, Denton, TX 76203, USA
[2]Magnesium Elektron North America Inc., Madison, IL 62060, USA
[3]U.S. Army Research Laboratory, Materials and Manufacturing Science Division, Aberdeen Proving Ground, MD 21005, USA

Keywords: Friction stir welding, Strain rate, Dynamic recrystallization, Joint efficiency, Stir Zone (SZ)

Abstract

The initial microstructure plays an important role in determining the spatial and temporal evolution of the microstructure during friction stir welding (FSW). The overall kinetics of microstructural evolution is location sensitive and the effect of the process strain, strain rate and thermal cycle creates complexities. In the present study, magnesium based WE43 alloy has been welded employing two different welding conditions. Joint efficiency has been subsequently evaluated. The results have been correlated with detailed microstructural information obtained from SEM and OIM-EBSD. The influence of microstructural evolution on strength has been analyzed. This framework provides an approach to maximize joint efficiency.

Introduction

The onset of many desirable features like fuel efficiency and high specific strength are driving Mg alloys towards potential structural applications in the future. Strengthening is often a key property for material selection in a majority of applications. As a result, the specific strength advantage of the Mg alloys over their counterparts has triggered intensive effort for their use in engineering applications. WE43 is currently touted to be one of the most promising Mg alloys due to its good elevated temperature properties, creep performance, flammability resistance and relatively higher strength [1,2]. However, welding of Mg alloys is a major challenge and limits the ability to fabricate large and complex components [3]. Therefore, joint efficiency can have significant impact on expanding its applicability towards various sectors in the near future. Extensive study on Al alloys and a lucid understanding of microstructural evolution during the friction stir process has been formulated and is available in the literature [4,5]. Starting from Al alloys, a variety of Mg alloys have also been studied.

Feng et al. [6] studied the effect of friction stir processing(FSP) on an AZ91 alloy and reported the dissolution and breakup of coarse eutectic $Mg_{17}Al_{12}$ phase. Park et al. [7] demonstrated the importance of texture and related it to the mechanical properties of an AZ61 alloy subjected to FSP. Ma et al. [8] suggested that FSP plays the role of solution treatment in AZ91 and saves time. Cao et al. [9] reported values of 69-78% for joint efficiencies in an AZ31-H24 alloy with failure occurring predominantly between stir zone(SZ) and thermo mechanically affected

zone(TMAZ). Several studies has been completed on the precipitation strengthened Mg alloys and indicate a strong dependency of strength on the evolution of strengthening precipitates [10,11,12,13] However, there is a strong demarcation with respect to the global value of strength, contributing factors and evolution path as a function of alloy chemistry during FSW. The thermal stability of the precipitates strongly determines the process conditions to be employed for achieving a desired microstructure. In comparison to the dissolution of precipitates in the AZ series, strengthening in Mg-Al-Ca and rare earth containing alloys like GWZ and WE43 is determined by the ability to control the intermetallic phases [6,11,12,13].
Freeney et al. [12] showed enhancement of the mechanical properties by breakage and dissolution of the second phases in a cast EV31 alloy. Xiao et al. [11] showed a large increase in the strength of a cast GW103 alloy after post FSP ageing. This was achieved by dissolving the Mg_5Gd intermetallics during processing. However, Zhang et al. [13] showed that the breakage and homogeneous distribution of Al_2Ca increased the strength and recommended faster welding speeds and lower heat input. Considering a variety of intermetallics (Mg_2Y, $Mg_{24}Y_5$, $Mg_{41}Nd_5$) that form in a WE43 alloy during casting and remain during subsequent shaping operations, it is interesting to study their response as a function of welding parameters [14,15,16]. Investigations indicate that different starting tempers can have significant impact during processing and result in different final values of strength. Freeney et al. [17] studied the effect of FSP on a cast WE43 alloy and obtained a nugget strength equivalent to 120% of the base material. Though a large extent of literature exists on the friction stir welding of Mg alloys, the industrially important WE43 alloy has not been evaluated much. To the best of our knowledge, no report exists on the microstructure-joint efficiency relationship in a wrought WE43 alloy.

The present study aims at correlating the effect of process parameters on the microstructure and mechanical property of a T5 temper WE43 alloy.

Experimental Details

For this study, 3.5 mm thick sheets of WE43 alloy in the rolled condition was provided by Magnesium Elektron. The nominal composition of the alloy was 4% Y-3% Nd-0.5% Zr–bal Mg (all in wt%). The alloy was subjected to ageing at 210 ^{0}Cfor 48h to maximize the base strength. The samples were longitudinally friction stir welded by employing a conical threaded pin made of tool steel with a concave shaped featureless shoulder. The pin height, pin diameter at the tip and root of the pin were 1.4 mm, 3.4 mm and 5.6 mm, respectively. A single pass FSW was performed at tool rotation rates of 600 and 800 rpm and a constant traverse speed of 102 mm/min.

The specimens for microstructural examination were cross sectioned perpendicular to the FSW direction. A standard sequential metallurgical procedure such as cutting, mounting and polishing with alcohol based diamond polishing compound was employed. Structural features were subsequently revealed by etching for duration of 10s in a mixture of acetic glycol (20 mL), (1 mL) HNO_3, (60 mL) ethylene glycol, and (20 mL) water, and washing with ethanol. Microstructural analysis and characterization was extensively carried out by employing a scanning electron microscope (FEI Nova NanoSEM 230). Samples for EBSD analysis were prepared using diamond based compounds to a final polishing step of 0.02 μm. These samples were subsequently electro-polished (40% H_3PO_4 and 60% ethanol at 20°C) using a voltage of 2–

3V for 10–15s and washed using ethanol. A FEI Nova NanoSEM 230 (20 kV, 3.1 mA, tilting 70^{o}, 0.3 µm step size) was used to record the EBSD patterns for stir zone.

The Vickers microhardness measurements were done at a load of 1.961 N with a 10 s dwell time. These measurements were performed through the center of the transverse cross section in the SZ and extending into the base matrix on either sides for a distance of 15 mm. Quantitative analysis was done using the ImageJ software package. The grain size determination was done using the linear intercept method.

Results and Discussion

Initial microstructure: As rolled + T5

The as-rolled microstructure was subjected to ageing based on the optimal conditions reported in literature. This heat treatment has been reported to precipitate strengthening β" and β' phases [18,19,20]. Extensive analysis of the microstructure depicted three interesting features: shear bands, intermetallic clusters of RE and precipitation gradients. Fig (1a) shows patches of inhomogeneity in the rolled structure suggesting preferential shear localization during rolling. Jin et al. [21] studied the deformation behavior of a coarse grained AZ31 alloy and observed such inhomogeneous structures. The observation was reasoned based on dissimilar recrystallization magnitude of different grains owing to their orientation with respect to the compressive stress. Serajzadeh et al. [22] employed modeling and related the microstructural inhomogeneity to the inherent and inevitable strain gradients. The study also suggested that the extent of inhomogeneity would be directly proportional to the reduction per pass. In the present case, a greater reduction per pass at lower temperature substantiates the microstructural features. Another plausible reasoning could be the persistence of the solute that segregated to the interdendritic spaces during solidification. This mechanism of chemical partitioning can lead to a local supersaturation and subsequent precipitation of non-strengthening precipitates. Thus, the prior microstructure plays a crucial role in the subsequent evolution of microstructure and mechanical variables during isothermal ageing. The average grain size was 35±15 µm.

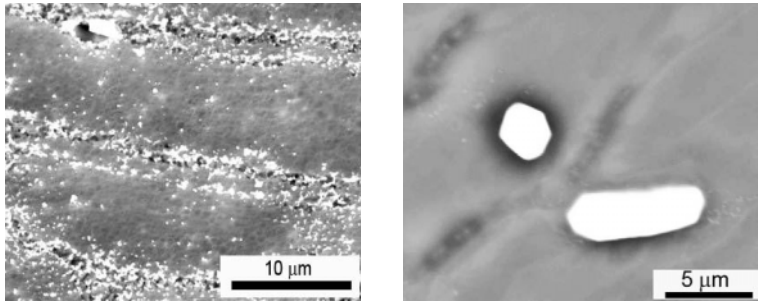

Fig. 1. (a) SE micrograph depicting shear localization and precipitation gradients (b) BSE micrograph showing cuboidal $Mg_2YZr_{0.3}$ and plate shaped $Mg_{41}Nd_5Zr$ intermetallics

Fig. 1(b) shows the presence of large cuboidal intermetallic of Mg_2Y and plate like $Mg_{41}Nd_5$.

These intermetallics have been reported to form during the solidification stage and persisted during subsequent rolling operations [14-15]. Such cuboidal precipitates have been reported by numerous researchers in Gd containing alloys [11]. High thermal stability of these precipitates has been reported and their melting point has been quoted to be around 620 ^{0}C.The presence of such coarse particles(~4-5 µm) would be inefficient in serving as an obstacle to dislocation motion. Therefore, it would be interesting to note the behavior of these particles subjected to FSW.

FSW

This study aims at reasoning the evolution of microstructure as a function of welding parameters and resultant thermal cycle. The major contributing factors to strengthening in a WE43 alloy are grain size and precipitate descriptors. Therefore, it is necessary to understand the competing aspects of strain, strain rate and temperature. The deformation strain, peak temperature and the grain size are correlated employing the Zener-Holloman parameter, Z (s^{-1}). Table I summarizes the mathematical equations employed to establish the Zener-Holloman parameter from the literature.

Table I. Equations for process parameters based calculations [23-26].

$Z = \dot{\varepsilon}\ \exp\left(\frac{Q}{RT}\right)$ (1)	$\varepsilon = ln\left(\frac{l}{APR}\right) + \left\lvert ln\left(\frac{APR}{l}\right)\right\rvert$ (2)	$l = 2r\cos^{-1}\left[\frac{r-x}{r}\right]$ (3)
$\dot{\varepsilon} = \varepsilon/t$ (4)	$l = \frac{\mathrm{APR}}{v}$ (5)	$\ln d = A1 - A2\ln Z$ (6)

where $\dot{\varepsilon}$ is the strain rate, R the gas constant, T the temperature, Q the activation energy, l the maximum deformed length, APR the tool advance per revolution, r the tool pin radius, x the perpendicular distance to welding direction from retreating side to advancing side of the tool, v the welding speed (mm s^{-1}) and d is the grain size.

The peak temperature is determined by employing the Arbegast empirical relationship: [27]

$$\frac{T}{T_m} = K\left(\frac{\omega^2}{2.362v \times 10^4}\right)^{\alpha} \quad (7)$$

Where, T_m is the melting temperature (893 K for WE43), ω the tool rotation rate(rpm.) and v the tool traverse speed(mm s^{-1}). In the present study the values of K and α were averaged over the reported values by Chang et al. [28] and Commin et al. [29] for AZ 31 and Mg alloys. The activation energy was assumed to be the lattice diffusion of Mg and taken to be 135 $Jmol^{-1}$. Table II summarizes the process parameter based calculations employing equations from Table I.

Table II. Summary of process parameter based calculations.

Rotational speed (RPM)	Welding speed (mm/min)	Strain	Strain rate (s^{-1})	Peak temperature (K)	Zener-Holloman parameter, Z (s^{-1})
600	102	8.0	80	621	2×10^{13}
800	102	8.6	115	660	6×10^{12}

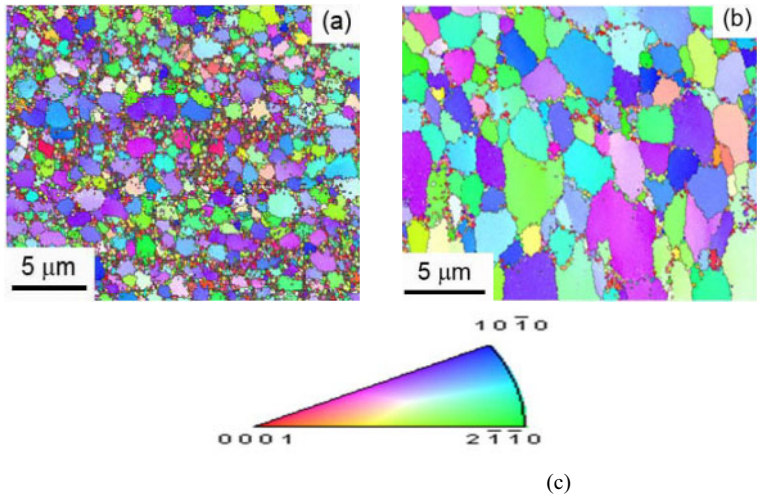

(c)

Fig. 2. EBSD micrographs of (a) 600/102, (b) 800/102 and (c) IPF color code

Examination of OIM micrographs reveal fine grained structures indicating extensive dynamic recrystallization. This is indicative of extremely high deformation rates calculated in Table II. Figures 2(a) and (b) show the grain size in specimens welded at 600/102 and 800/102 to be around 1.7 and 2.7, μm respectively. This observation can be rationalized based on the Z parameter and peak temperature. A welding parameter of 600/102 results in a lower peak temperature and a higher Z parameter. In comparison to the 800/102 sample, the increase in the Z magnitude for a 600/102 sample by an order results in a finer grain size. Freeney et al. [13] reported the grain size to be 6.1 μm for a cast EV31A processed at 400/102. Investigations for a T5 WE43 shows a grain size of 1.5-2.5 μm subjected to a higher heat input as compared to EV31A. A higher grain refining sensitivity in a WE43 alloy could be reasoned based on a greater extent of second phases and Zr content that would impact pinning and higher extent of solute elements. In comparison to the cast WE43 alloy processed at 400/102, T5 temper exhibited a finer grain size substantiating the importance of initial microstructure. Though, DRX is unanimously accepted, there is a conflict over the mechanistic mode triggering recrystallization.

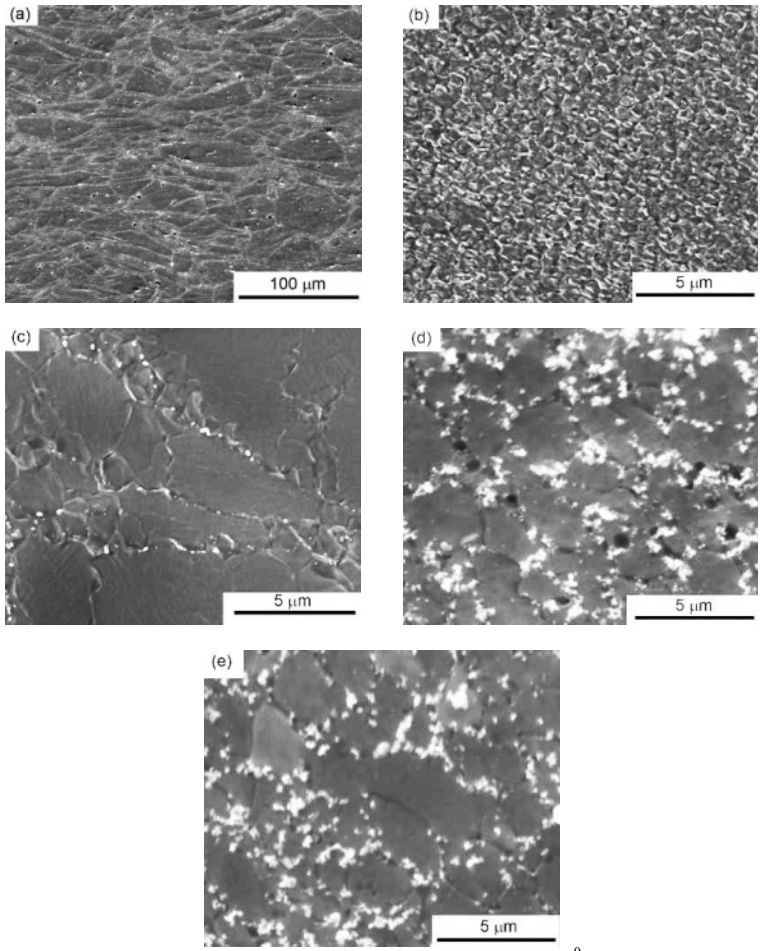

Fig. 3. SEM micrographs of different conditions ; (a) AR+T5 (210 ^{0}C/48h), (b) 600/4 SZ, (c) 600/102 TMAZ, (d) 800/102 SZ, (e) 800/102 TMAZ

Figures 3 (a-e) indicate the various zones and the characteristic features embedded in the microstructure obtained from SEM examination. The area fraction of the precipitates was evaluated using imageJ and decreased from 24.1% in the T5 state to 16.1 and 17.4% in 600/102 and 800/102, respectively. Friction stir welding has led to partial homogenization as compared to the T5 condition (Figs. 3b and d). For a sample processed at a higher rotational rate (Fig. 3d), it

showed preferential precipitate coarsening at the grain boundaries as compared to 600/102. Since coarsening is dependent on the thermal profile and mechanical cycle, the evolution becomes a complex function of the competing factors. For an 800/102 sample, the peak temperature is above the dissolution temperature of strengthening precipitates and would soften the matrix to a greater extent. Non-equilibrium reprecipitation would then favor the formation of non-strengthening β precipitates at grain boundaries. Figs. 3(c) and (e) depict formation of necklace structures and fragmentation of prior grains leading to finer grains by recrystallization and break up. This is due to high bulk diffusivity of Mg at a particular temperature in comparison to Al alloys.

Mechanical properties and effect of Post weld heat treatment (PWHT)

Differences exhibited by 600/102 (Fig. 3b) and 800/102 (Fig. 3d) in terms of precipitate characteristics and grain size markedly affected the strength levels, by 6-7 HV in the HAZ, and by 5 HV in the nugget as shown in Fig. 4 (a). A W shaped curve was observed and can be reasoned based on the effect of shoulder. The shoulder diameter (d)/Sheet thickness (t) ratio was approximately three resulting in greater accumulation of heat. This is analogous to a heat pumping source possessing a greater temperature field over a smaller distance. Thus the HAZ would experience higher temperatures with a knockdown in properties. PWHT increased the SZ, TMAZ and HAZ strength and marginally lowered the strength of the base metal. Therefore, the joint efficiency values considerably increased after aging.

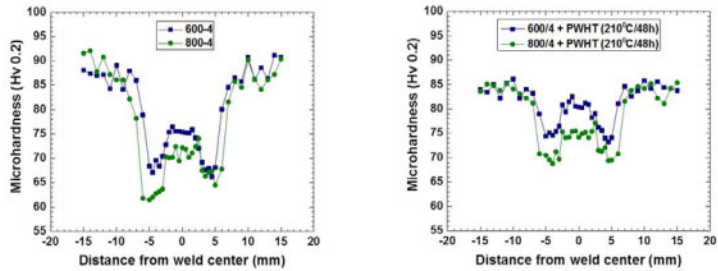

Fig. 4. Microhardness data for as processed and PWHT samples.

4. Conclusions

The effect of processing conditions on the joint efficiency of a T5 temper WE43 alloy was investigated. Based on the study, the following conclusions are made:

1) The FSW of WE43 resulted in grain refinement, breakage and dissolution of second phase particles leading to homogenization. The grain size reduced from 35 ± 15 μm in the T5 state to 1.7 ± 0.2 μm and 2.7 ± 0.26 μm in a 600/102 and 800/102 samples.
2) The shoulder diameter to sheet thickness ratio was 3 resulting in a concentrated temperature field. This lead to a wide HAZ extending from the periphery of the TMAZ to the base metal.
3) The HAZ served as the weakest link with a joint efficiency of 73.5% and 67% for a 600/102 and 800/102 samples. These values increased to 85 and 79.5% after PWHT respectively. A

better understanding of microstructure evolution coupled with aging optimization needs to be done.

5. References

1. B.L Mordike, "Development of highly creep resistant Magnesium alloys," Journal of Materials Processing and Technology, 117 (2001), 391-394.
2. I.J Polmear, "Recent development in light alloys," Materials transactions, 36 (1996), 12-31.
3. Frank Czerwinski, "Welding and Joining of Magnesium Alloys," Magnesium alloys-Design, processing and properties (intechopen.com).
4. A. Simar, Y. Bréchet, B. de Meester, A. Denquin, C. Gallais, T. Pardoen, "Integrated modeling of friction stir welding of 6xxx series Al alloys: Process, microstructure and properties," Progress in Materials Science 57 (2012), 95-183.
5. Threadgill PL, Leonard AJ, Shercliff HR, Withers PJ, "Friction stir welding of aluminium alloys," Int Mater Rev 54 (2009), 49–93.
6. A.H. Feng and Z.Y. Ma, "Enhanced mechanical properties of Mg–Al–Zn cast alloy via friction stir processing," Scripta Materialia 56 (2007), 397–400.
7. Seung Hwan C. Park, Yutaka S. Sato, Hiroyuki Kokawa, "Effect of micro-texture on fracture location in friction stir weld of Mg alloy AZ61 during tensile test," Scripta Materialia 49 (2003), 161–166.
8. Z.Y. Ma, A.L. Pilchak, M.C. Juhas, J.C. Williams, "Microstructural refinement and property enhancement of cast light alloys via friction stir processing," Scripta Materialia 58 (2008), 361–366.
9. X. Cao, M. Jahazi, "Effect of welding speed on the quality of friction stir welded butt joints of a magnesium alloy," Materials and Design 30 (2009), 2033–2042.
10. G.M. Xie , Z.Y. Ma, L. Geng, "Effect of microstructural evolution on mechanical properties of friction stir welded ZK60 alloy," Materials Science and Engineering A 486 (2008), 49–55.
11. B.L. Xiao, Q. Yang, J. Yang, W.G. Wang, G.M. Xie, Z.Y. Ma, "Enhanced mechanical properties of Mg–Gd–Y–Zr casting via friction stir processing," Journal of Alloys and Compounds 509 (2011), 2879–2884.
12. T.A. Freeney, R.S. Mishra, "Effect of Friction Stir Processing on Microstructure and Mechanical Properties of a Cast-Magnesium–Rare Earth Alloy," Metallurgical and Materials Transactions 41A (2010), 73-84.
13. Datong Zhang, Mayumi Suzuki, Kouichi Maruyama, "Microstructural evolution of a heat-resistant magnesium alloy due to friction stir welding," Scripta Materialia 52 (2005), 899–903.
14. Zaijun Su, Chuming Liu, Yingchun Wan, "Microstructures and mechanical properties of high performance Mg-4Y-2.4Nd-0.2Zn-0.4Zr alloy," Materials and Design (2012).
15. Kun Yu, Wenxian Li, Richu Wang, Bo Wang, Chao Li, "Effect of T5 and T6 Tempers on a Hot-Rolled WE43 Magnesium Alloy," Materials Transactions 49 (2008), 1818 -1821.
16. R. Arrabal, E. Matykina, F. Viejo, P. Skeldon, G.E. Thompson, "Corrosion resistance of WE43 and AZ91D magnesium alloys with phosphate PEO coatings," Corrosion Science 50 (2008), 1744-1752.
17. T.A. Freeney, R.S. Mishra, G.J. Grant, and R. Verma, "Friction Stir Welding and Processing IV, TMS, Warrendale," PA, 2007.

18. P. Mengucci, G.Barucca, G. Riontino, D. Lussana, M. Massazza, R. Ferragut, E. Hassan Aly, “Structure evolution of a WE43 Mg alloy submitted to different thermal treatments,” Materials Science and Engineering A 479 (2008), 37-44.
19. Renlong Xin, Ling Li, Ke Zeng, Bo Song, Qing Liu, “Structural examination of aging precipitation in a Mg-Y-Nd alloy at different temperatures,” Materials Characterization 62 (2011), 535-539.
20. J.F Nie, B.C Muddle, “Characterisation of strengthening precipitate phases in a Mg-Y-Nd alloy,” Acta mater. 48 (2000), 1691-1703.
21. Qinglin Jin, Sung-Yong Shim and Su-Gun Lim, “Correlation of microstructural evolution and formation of basal texture in coarse grained Mg-Al alloy during hot rolling,” Scripta Materialia 55 (2006), 843-846.
22. S. Serajzadeha, A. Karimi Taheria, M. Nejatib, J. Izadib, M. Fattahi, “An investigation on strain inhomogeneity in hot strip rolling process,” Journal of Materials Processing Technology 128 (2002), 88–99.
23. Myshlyaev, M.M., McQueen, H.J.,Mwembela, A. Konopleva, E., “Twinning, dynamic recovery and recrystallization in hot worked Mg–Al–Zn alloy,” Materials Science and Engineering A, 337 (2002), 121-133.
24. K.Dehghani, A. Chabok, “Dependence of Zener parameter on the nanograins formed during friction stir processing of interstitial free steels,” Materials Science and Engineering A, 528 (2011), 4325-4330.
25. A.P Reynolds, “Flow visualization and simulation in FSW, Scripta Materialia,” 58 (2008), 338-342.
26. M. Ghosh, K. Kumar, R.S. Mishra“Analysis of microstructural evolution during friction stir welding of ultrahigh-strength steel,” Scripta Materialia, 63 (2010), 851-853.
27. W.J. Arbegast, “Hot Deformation of Aluminum Alloys III,” TMS, Warrendale, PA (2003).
28. C.I Chang, C.J. Lee, J.C. Huang, “Relationship between grain size and Zener–Holloman parameter during friction stir processing in AZ31 Mg alloys,” Scripta Materialia, 51 (2004), 509-514.
29. L. Commin, M. Dumont, J.E. Masse, L. Barrallier, “Friction stir welding of AZ31 magnesium alloy rolled sheets: Influence of processing parameters,” Acta Materialia, 57 (2009), 326-334.

NO. OF COPIES	ORGANIZATION
1 (PDF)	DEFENSE TECHNICAL INFORMATION CTR DTIC OCA 8725 JOHN J KINGMAN RD STE 0944 FORT BELVOIR VA 22060-6218
1 (PDF)	DIRECTOR US ARMY RESEARCH LAB RDRL CIO LL 2800 POWDER MILL RD ADELPHI MD 20783-1197
1 (PDF)	GOVT PRINTG OFC A MALHOTRA 732 N CAPITOL ST NW WASHINGTON DC 20401
1 (PDF)	RDRL WMM F K DOHERTY